Coherent control of the photoinduced transition in a strongly correlated material

Eduardo B. Molinero [1,*] and Rui E. F. Silva [1,2,†]

[1]*Instituto de Ciencia de Materiales de Madrid, Consejo Superior de Investigaciones Científicas (ICMM-CSIC), E-28049 Madrid, Spain*
[2]*Max-Born-Institut, Max Born Strasse 2A, D-12489 Berlin, Germany*

(Received 14 June 2022; revised 3 October 2022; accepted 18 November 2022; published 19 December 2022)

The use of intense tailored light fields is the perfect tool to achieve ultrafast control of electronic properties in quantum materials. Among them, Mott insulators are materials in which strong electron-electron interactions drive the material into an insulating phase. When shining a Mott insulator with a strong laser pulse, the electric field may induce the creation of doublon-hole pairs, triggering a photoinduced transition into a metallic state. In this paper, we take advantage of the threshold character of this photoinduced transition and we propose a setup that consists of a midinfrared laser pulse and a train of short pulses separated by a half period of the midinfrared with alternating phases. By varying the time delay between the two pulses and the internal carrier envelope phase of the short pulses, we achieve control of the phase transition, which leaves its fingerprint at its high harmonic spectrum.

DOI: 10.1103/PhysRevResearch.4.043198

I. INTRODUCTION

The desire for controlling the quantum properties of matter is a common trend between many scientific disciplines, with the field of femtochemistry being the most well-known example [1]. Modern advances both in laser technology, which make it possible to control the laser properties within each laser cycle [2–4], alongside improvements in materials science, have paved the way to obtain coherent control over quantum materials. Prominent examples include controlling the valley degrees of freedom [5] and topological properties [6] of two-dimensional (2D) materials, inducing coherent spin switching [7] and structural phase transitions [8,9], and lastly, the possibility of accomplishing petahertz electronics [10,11].

Light sources may not only give us control over quantum properties, but also induce exotic and novel states of matter which are the result of purely nonequilibrium phenomena, and hence their mechanisms are radically distinct from those in equilibrium [12,13]. For instance, there has been a lot of recent interest in photoinduced insulator-to-metal transitions in a variety of strongly correlated materials [14–17]. Their common underlying physical phenomenon is photodoping, i.e., an abrupt change in the concentration of charge carriers due to the presence of a strong laser field, without any modification to its chemical composition. In the case of Mott insulators, the ground state is photoinduced into an excited one, characterized by the presence of pairs of doublons (double occupation in a given site) and holes (no occupation).

This dielectric breakdown of Mott insulators has not only been studied theoretically using various methods such as exact diagonalization [18,19], time-dependent density matrix renormalization group [20–23], and nonequilibrium dynamical mean-field theory [24–28], but it has also been confirmed experimentally [29,30]. Owing to those works, it was revealed that the dielectric breakdown has a pronounced threshold character. In the case of one-dimensional Mott insulators, it was shown that the final metallic state was a photoinduced Tomonaga-Luttinger-like liquid [20,21].

More precisely, the laser can break the short-range antiferromagnetic order of the Mott insulator by favoring the appearance of the above-mentioned doublon-hole pairs. The mechanism behind this phenomenon is analogous to that present in strong field ionization in atoms [2]. In fact, one could define an adiabaticity parameter γ_K which plays the same role as the Keldysh parameter in atoms [31,32], defined as $\gamma_K = \hbar\omega_L/\xi F_0$, where ξ is the correlation length [21] and ω_L is the frequency of the laser. In the *tunneling* regime, $\gamma_K \ll 1$, an electron can tunnel through the interaction repulsion over a distance $\sim\xi$ due to the presence of the laser. Thus, a doublon-hole pair is formed, which leads to the melting of the insulator state [see Fig. 1(a)]. However, and due to its threshold character, this will only happen if the field goes higher than a certain value F_{th} [19,21]. In Mott-like systems, this threshold is given by $F_{\text{th}} = \Delta/2e\xi$, where Δ is the Mott gap. Recent works have shown that this ulfrafast photoinduced transition can be time resolved owing to its high harmonic emission [19,33,34].

In this paper, we propose the use of a setup that consists of two lasers (a femtosecond pulse train and a midinfrared pulse) with a varying time delay between them [see Fig. 1(b)], that enables us to control the ultrafast photoinduced transition by taking advantage of its threshold behavior.

*ebmolinero@gmail.com
†rui.silva@csic.es, ruiefdasilva@gmail.com

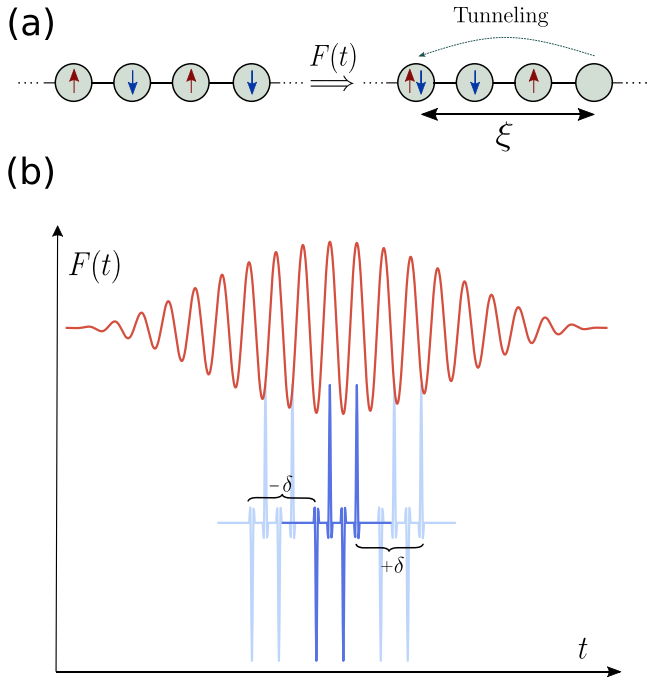

FIG. 1. (a) Schematic representation of the tunneling phenomenon in the 1D Fermi-Hubbard model. (b) Representation of the two different lasers. The red line denotes the mid-IR laser while the blue line corresponds to the train of short pulses with $\phi_{\rm CEP} = 0$. Lighter blue lines show how a $\pm\delta$ delay affects the train.

II. THEORETICAL FRAMEWORK

We will focus on the one-dimensional Hubbard model and we will use parameters to mimic Sr_2CuO_3. The main purpose of the present paper is to show that one can take advantage of this tunneling phenomenon, to acquire a coherent control over the photoinduced transition from an insulating state into a metallic one in a strongly correlated material.

In order to model the dynamics, we consider the one-dimensional Hubbard model,

$$H = -\tau \sum_{j=1,\sigma}^{L} (e^{-i\Phi(t)} c^{\dagger}_{j,\sigma} c_{j+1,\sigma} + \text{H.c.}) + U \sum_{j=1}^{L} n_{j,\uparrow} n_{j,\downarrow}, \tag{1}$$

where $c^{\dagger}_{j,\sigma}$ ($c_{j,\sigma}$) is the fermionic creation (annihilation) operator for site j and spin σ and $n_{j,\sigma} = c^{\dagger}_{j,\sigma} c_{j,\sigma}$ is the number operator. The physical parameters τ and U have been set to $\tau = 0.52$ eV and $U = 5.96\tau$ to mimic Sr_2CuO_3 [21], which also ensures us that we are in the strong-coupling limit, i.e., $U \gg \tau$. We will focus on the half-filling case (one electron per site). In this case, the ground state (also referred to as the Mott insulator) has a short-range antiferromagnetic order [35]; the electrons become localized in position space with antiparallel spins respective to their adjacent sites. The laser electric field $F(t)$ is taken into account through the Peierls phase [35]: $d\Phi(t)/dt = -eaF(t)$, where $a = 7.56$ a.u. is the lattice constant of Sr_2CuO_3 and e is the electron charge. We will solve it using $N = L = 12$, setting periodic boundary conditions ($c_{j+L,\sigma} = c_{j,\sigma}$) and focusing on the $S_z = 0$ subspace. Our approach consists of exactly solving the time-dependent Schrödinger equation (TDSE) using a time step of $dt = 0.5$ a.u. In order to check for possible finite-size artifacts, we have calculated ξ for our system [36]. We obtained a value of $\xi \simeq 2a$, which therefore implies that finite-size corrections are negligible. Furthermore, convergence with the number of sites was checked by performing calculations for $N = L = 10$, 12, 14.

As previously mentioned, we will use two different lasers and tune the time delay δ between them in order to obtain control. The first will consist of a mid-IR laser with frequency $\omega_{\rm IR} = 32.92$ THz and an amplitude of $F_{0,\rm IR} = 5$ MV/cm. The second laser will be a train made up of four short pulses (their total duration is roughly 6 fs) equally split. The time delay between two consecutive short pulses is a half period of the mid-IR laser pulse and they have alternating phases, in accordance to what is obtained by means of high harmonic generation [resembling a reconstruction of attosecond beating by interference of two-photon transitions (RABBIT) scheme [37–39]]. The parameters for the short pulses are $\omega_{\rm pul} = 5\omega_{\rm IR} = 164.6$ THz, having a central frequency that corresponds to the fifth harmonic, and an amplitude of $F_{0,\rm pul} = 8$ MV/cm. Both lasers are modulated by a $\cos^2$ envelope [40] as it can be appreciated in Fig. 1(b). Nevertheless, we found that the physics described here are robust to changes in the envelope function. If one defines a single laser pulse as

$$\begin{aligned} &E(t, t_0, T, \omega, E_0, \phi) \\ &\quad = E_0 \cos^2[\pi (t - t_0) T^{-1}] \\ &\qquad \times \theta(0.5T - |t - t_0|) \cos[\omega(t - t_0) + \phi], \end{aligned} \tag{2}$$

the two-laser setup used is given by

$$\begin{aligned} F(t) = {} & E(t, 0, 20T_{\rm IR}, \omega_{\rm IR}, F_{0,\rm IR}, \pi/2) \\ & + \sum_{n=1}^{4} E(t, t_{0,n}, T_{\rm pul}, \omega_{\rm pul}, F_{0,\rm pul}, \phi_{\rm CEP} - n\pi), \end{aligned} \tag{3}$$

where $\omega_{\rm IR} = 32.92$ THz is the frequency of the mid-IR pulse ($T_{\rm IR} = 2\pi/\omega_{\rm IR}$), $\omega_{\rm pul} = 5\omega_{\rm IR}$ is the central frequency of the single-cycle femtosecond pulses ($T_{\rm pul} = 2\pi/\omega_{\rm pul}$), $F_{0,\rm IR} = 5$ MV/cm is the amplitude of the mid-IR pulse, $F_{0,\rm pul} = 8$ MV/cm is the amplitude of the single-cycle femtosecond pulses, $t_{0,n} = [(2n-5)/4]T_{\rm IR} + \delta/\omega_{\rm IR}$, δ is the delay between the two pulses in radians, and $\phi_{\rm CEP}$ is the carrier envelope phase of the single-cycle femtosecond pulses. The threshold field [21] for Sr_2CuO_3 takes a value of $F_{\rm th} = 9.1$ MV/cm so neither of the fields can surpass it on their own; only when the two amplitudes sum in a coherent way, namely when the short pulses land right on the peaks of the mid-IR, will the electric field break the threshold, and thus the transition will take place. The specific delays in which this will occur will heavily depend on $\phi_{\rm CEP}$ of the short pulses. For example, by looking at Fig. 1(b) one can easily guess that for $\phi_{\rm CEP} = 0$, the two lasers will sum coherently at $\delta = 0$. As a result, we can *control the photoinduced transition* by light-wave engineering of the two parameters δ and $\phi_{\rm CEP}$. It must be emphasized that these laser parameters are well within experimental reach.

To characterize the photoinduced transition, one must pay attention to both charge and spin degrees of freedom. To do so, we will compute the following observables in the Schrödinger

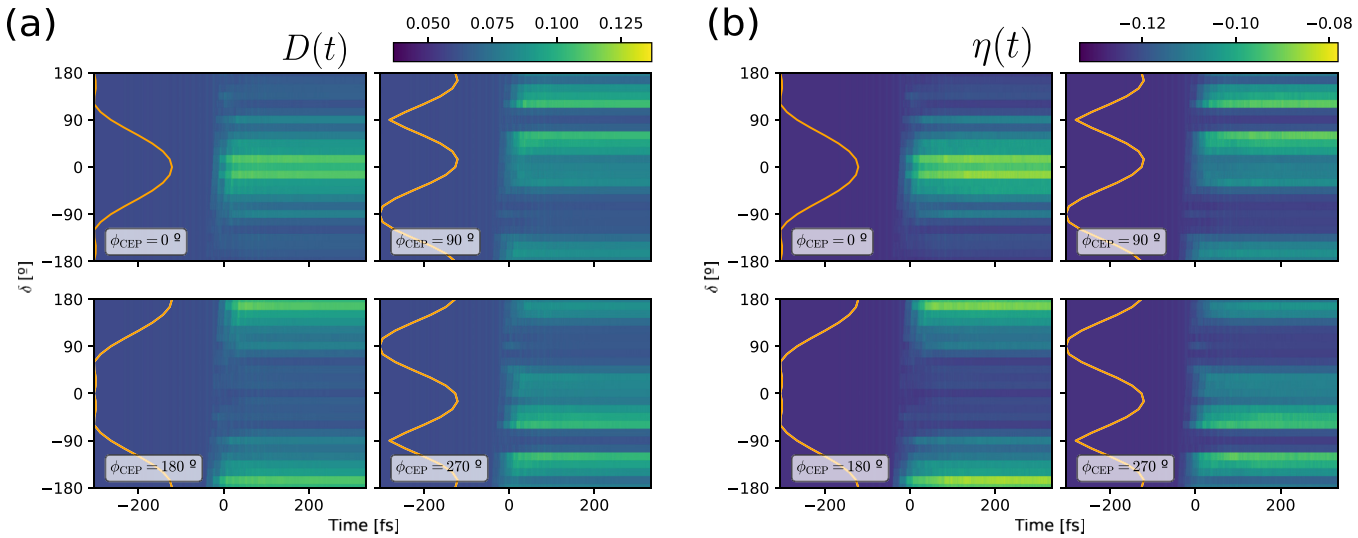

FIG. 2. (a) Average number of doublon-hole pairs $D(t)$ and (b) next-neighbor spin-spin correlation function $\eta(t)$, as a function of time and δ, for different values of $\phi_{\rm CEP}$. The values shown are convoluted with a normal distribution function with $\sigma = 1$ fs. The orange line shows the total production rate Γ obtained for the corresponding delay. The carrier envelope phase (CEP) of the laser is shown inside each figure.

picture: first, the average number of doublon-hole pairs

$$D(t) = \frac{1}{L}\sum_j \langle n_{j,\uparrow} n_{j,\downarrow}\rangle, \tag{4}$$

and second, the next-neighbor spin-spin correlation function

$$\eta(t) = \frac{1}{L}\sum_j \langle \vec{S}_j \cdot \vec{S}_{j+1}\rangle, \tag{5}$$

where $\vec{S}_j$ is the vector of spin matrices for spin-1/2 and site j.

At first, it may seem that predicting for which values of δ and $\phi_{\rm CEP}$ the phase transition takes place can be quite a task. However, we can accomplish this by just computing the maximum production rate Γ of the doublon-hole pairs in *the tunneling regime*. Following Ref. [21], we take the production rate as

$$\Gamma = \exp\left(-\pi \frac{F_{\rm th}}{\max|F(t)|}\right). \tag{6}$$

Therefore, only by knowing the shape of the laser and the threshold amplitude (which depends solely on the material) can we make a very confident guess of the nonequilibrium behavior of the material. It must be noted that this rough estimation is only valid when we are in the tunneling regime. By calculating the adiabaticity parameter for both pulses separately, we found that $\gamma_{K,\rm pul} = 1.03$ and $\gamma_{K,\rm IR} = 0.33$. The mid-IR pulse is well in the tunneling regime and the train pulse is in the frontier between the multiphoton and tunneling regime. However, when calculating $\gamma_{K,\rm pul}$, summing the two field strengths we get $\gamma_{K,\rm pul} = 0.63$, which is indeed in the tunneling regime. Consequently, Γ as defined in Eq. (6), for our laser parameters, can be used as a good number, indicating whether or not we are inducing the dielectric breakdown.

III. RESULTS

To prove the above assumptions, we have performed several numerical calculations. In Fig. 2(a) we can see that the profile of $D(t)$ coincides almost perfectly with the prediction given by Γ. When the production rate starts to increase, i.e., when the delay δ (and the $\phi_{\rm CEP}$) causes the field to fulfill $\max|F(t)| > F_{\rm th}$, doublon-hole pairs begin to appear due to

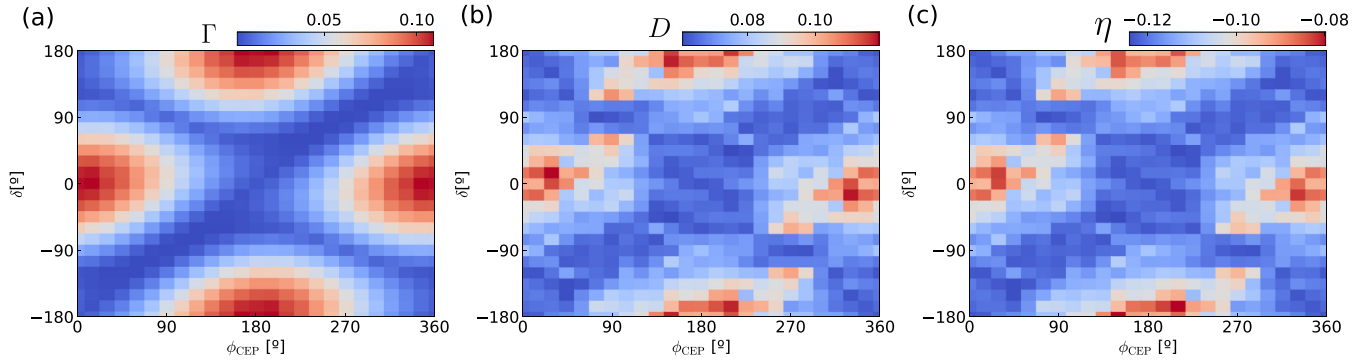

FIG. 3. (a) Total production rate Γ. Phase diagrams of (b) $D(t)$ and (c) $\eta(t)$. Both of these phase diagrams are obtained as the mean value of a 30 fs period of time after the end of the laser pulse.

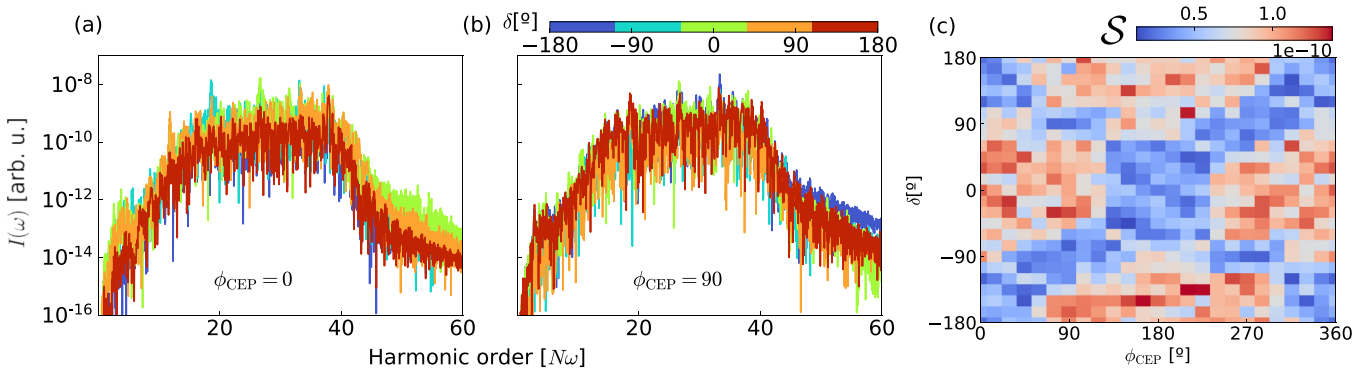

FIG. 4. Harmonic spectra in arbitrary units (a) for $\phi_{\rm CEP} = 0$ and (b) for $\phi_{\rm CEP} = 90$. We have included only five different delays in each plot for the sake of clarity. (c) Integrated spectrum $\mathcal{S}$ computed for the same range of δ and $\phi_{\rm CEP}$ as in Fig. 3.

the tunneling mechanism, and so the insulator state breaks down, leaving the system in a photoinduced saturated state [20,21]. On the other hand, when δ and $\phi_{\rm CEP}$ are such that the field does not surpass the threshold, the initial ground state is kept intact. The same trend can be appreciated for $\eta(t)$: The antiferromagnetic order of the Mott state begins to decrease when Γ becomes maximum and is conserved in the opposite case [Fig. 2(b)]. Both $D(t)$ and $\eta(t)$ display the same behavior because they are both signaling the appearance of a photoinduced transition. When doublon-hole pairs begin to populate the system, electrons will be less likely to have neighbors with an antialigned spin, because doublon-hole pairs are spinless excitations [35]. Despite the simplicity of Eq. (6), it does capture the physics of the system in a remarkable manner, predicting even abrupt changes in the phase of the system [Figs. 2(a) and 2(b) corresponding to the case $\phi_{\rm CEP} = 90°$]. This resemblance between Γ and the physical observables reaffirms that the dynamics of the system are heavily dominated by the tunneling mechanism.

The possibility of making accurate predictions, along with the tunability of the two parameters δ and $\phi_{\rm CEP}$, is what gives us *control over the transition* as shown in Fig. 3, where we have included Γ alongside a phase diagram of the system for a range of δ and $\phi_{\rm CEP}$. Comparing Fig. 3(a) with Fig. 3(b), one can see the clear correspondence between the theoretical prediction of the production rate and the obtained phase. As stated previously, when the production rate reaches a maximum, the system undergoes a dielectric breakdown, and if not, the system stays in the Mott insulator state. Nevertheless, and in spite of the similarities between these quantities (namely Γ vs D and η), they do not show exactly the same behavior. This is because tunneling is not a deterministic process but rather a probabilistic one; the electron is *not guaranteed* to tunnel over the potential barrier. Also, is worth noting the expected periodicity both in the delay and in the CEP.

However, measuring correlations in Mott-like systems is not an easy task [41]. Therefore, if we want to engineer the phase transition it is almost mandatory to find a more suitable figure of merit. Naturally, and since we are generating optical charge excitations, this process must manifest itself in the optical response of the system. Indeed, previous works have shown that a dielectric breakdown induced by strong laser fields leaves a fingerprint in the corresponding harmonic emission [19,33]. To compute the optical emission, we first obtain the electric current operator [35]

$$\hat{J}(t) = -iea\tau \sum_{j,\sigma} (e^{-i\Phi(t)} c^{\dagger}_{j,\sigma} c_{j+1,\sigma} - \text{H.c.}). \tag{7}$$

Afterwards, the harmonic spectra are computed through the Larmor's formula $I(\omega) \propto \omega^2 |\langle \hat{J}(\omega) \rangle|^2$, where $\hat{J}(\omega)$ is defined as the Fourier transform of the current operator using a limited-time window with a width of 1 fs. The spectrum (Fig. 4) displays the same features presented in Ref. [19]. The low intraband harmonics are mostly suppressed while the high harmonics are the most prominent. Furthermore, these are centered around the harmonic $N = U/\omega_L \sim 21$ as expected. However, if we compare the emission between different CEPs [Figs. 4(a) and 4(b)] there is no significant difference between $\phi_{\rm CEP} = 0°$ and $\phi_{\rm CEP} = 90°$. Additionally, varying the delay does not give a different spectra either.

However, if one now computes the integrated spectrum

$$\mathcal{S} = \int_{\omega_-}^{\omega_+} d\omega\, I(\omega), \tag{8}$$

a different behavior can be appreciated. We first note that the frequencies ω_+ and ω_- correspond to the upper and lower limits of the energy of the first allowed optical excitations [21,35], namely $\omega_- = \Delta$ and $\omega_+ = \Delta + 8\tau$. In Fig. 4(c) we have obtained $\mathcal{S}$ for the whole range of CEPs and delays, where we can see a noteworthy resemblance between that quantity and the prediction made in Fig. 3(a) using Γ. Therefore, we can also characterize the phase of the material owing to its optical response.

IV. CONCLUSION

One of the underlying assumptions of this paper is that electrons will maintain their coherence during the whole process. It has been shown that for bulk crystals, fast decoherence processes must be taken into account to match the experiments [42]. In those systems, dephasing is included *ad hoc*, so as to account for the many-body effects that go beyond the single-particle picture [43,44]. However, since the electron-electron interaction is one of the major causes of decoherence, which has been exactly included since the beginning, we hope that this phenomenon should be somewhat robust under dephasing effects.

Even though a dielectric breakdown also happens in uncorrelated semiconductors [45], the results presented in this paper are unique to strongly correlated systems. Although the emission spectra from both systems are already quite different [43], the major differences arise in the final state of the system. As mentioned before, the final state of the system is a photoinduced Tomonaga-Luttinger liquid [20,21], a completely distinct state when compared to a Mott-like one. There is no analog of this phenomenon in uncorrelated semiconductors.

As a prospect of future research, it could be interesting to see how the inclusion of dissipative degrees of freedom affects this process. Nevertheless, their effect should not affect the physics described here, essentially because relaxation processes (due to dissipation) and the photoinduced phase transition operate in different timescales; the former has a typical timescale of picoseconds [11,46] while the latter takes place in a few femtoseconds.

Our work has shown that it is possible to acquire control of a photoinduced transition in one-dimensional systems using electric fields. More specifically, we have shown that by superposing two different lasers, a mid-IR and a train of short pulses, the transition can be engineered by tuning the internal parameters of the lasers, the time delay between them and the internal carrier envelope phase of the short pulses (δ and ϕ_{CEP} in our case). Alongside this tunability, we proved that the total doublon-hole production rate Γ gives a simple, yet accurate, method of predicting the transition. Lastly, we found the existence of a more appropriate figure of merit to characterize the transition experimentally, by looking at the nonlinear optical response of the system. Accordingly, we can also characterize the photoinduced phase of the material using only its optical response, as opposed to other more sophisticated experimental setups, such as time-resolved angle-resolved photoemission spectroscopy [47].

This work may pave the way to experimental efforts in which a photoinduced transition in strongly correlated systems can be achieved in a coherent way using tailored laser pulses. Moreover, we expect that this coherent control can be also applied to systems with higher dimensions, since the dielectric breakdown of the material has exactly the same key properties in those systems [30,33].

ACKNOWLEDGMENTS

The authors acknowledge fruitful discussions with Álvaro Jiménez-Galán and Misha Ivanov. E.B.M. and R.E.F.S. acknowledge support from the fellowship LCF/BQ/PR21/11840008 from "La Caixa" Foundation (ID 100010434). This research was supported by Grant No. PID2021-122769NB-I00 funded by MCIN/AEI/10.13039/501100011033.

[1] A. H. Zewail, Femtochemistry: Atomic-scale dynamics of the chemical bond, J. Phys. Chem. A **104**, 5660 (2000).

[2] F. Krausz and M. Ivanov, Attosecond physics, Rev. Mod. Phys. **81**, 163 (2009).

[3] A. Wirth, M. T. Hassan, I. Grguraš, J. Gagnon, A. Moulet, T. T. Luu, S. Pabst, R. Santra, Z. A. Alahmed, A. M. Azzeer, V. S. Yakovlev, V. Pervak, F. Krausz, and E. Goulielmakis, Synthesized light transients, Science **334**, 195 (2011).

[4] O. Kfir, P. Grychtol, E. Turgut, R. Knut, D. Zusin, D. Popmintchev, T. Popmintchev, H. Nembach, J. M. Shaw, A. Fleischer, H. Kapteyn, M. Murnane, and O. Cohen, Generation of bright phase-matched circularly-polarized extreme ultraviolet high harmonics, Nat. Photonics **9**, 99 (2015).

[5] F. Langer, C. P. Schmid, S. Schlauderer, M. Gmitra, J. Fabian, P. Nagler, C. Schüller, T. Korn, P. G. Hawkins, J. T. Steiner, U. Huttner, S. W. Koch, M. Kira, and R. Huber, Lightwave valleytronics in a monolayer of tungsten diselenide, Nature (London) **557**, 76 (2018).

[6] Á. Jiménez-Galán, R. E. F. Silva, O. Smirnova, and M. Ivanov, Lightwave control of topological properties in 2D materials for sub-cycle and non-resonant valley manipulation, Nat. Photonics **14**, 728 (2020).

[7] S. Schlauderer, C. Lange, S. Baierl, T. Ebnet, C. P. Schmid, D. C. Valovcin, A. K. Zvezdin, A. V. Kimel, R. V. Mikhaylovskiy, and R. Huber, Temporal and spectral fingerprints of ultrafast all-coherent spin switching, Nature (London) **569**, 383 (2019).

[8] M. Rini, R. Tobey, N. Dean, J. Itatani, Y. Tomioka, Y. Tokura, R. W. Schoenlein, and A. Cavalleri, Control of the electronic phase of a manganite by mode-selective vibrational excitation, Nature (London) **449**, 72 (2007).

[9] J. G. Horstmann, H. Böckmann, B. Wit, F. Kurtz, G. Storeck, and C. Ropers, Coherent control of a surface structural phase transition, Nature (London) **583**, 232 (2020).

[10] J. Schoetz, Z. Wang, E. Pisanty, M. Lewenstein, M. F. Kling, and M. F. Ciappina, Perspective on petahertz electronics and attosecond nanoscopy, ACS Photonics **6**, 3057 (2019).

[11] S. Y. Kruchinin, F. Krausz, and V. S. Yakovlev, Colloquium: Strong-field phenomena in periodic systems, Rev. Mod. Phys. **90**, 021002 (2018).

[12] K. Nasu, *Photoinduced Phase Transitions* (World Scientific, Singapore, 2004).

[13] D. N. Basov, R. D. Averitt, D. van der Marel, M. Dressel, and K. Haule, Electrodynamics of correlated electron materials, Rev. Mod. Phys. **83**, 471 (2011).

[14] S. Iwai, M. Ono, A. Maeda, H. Matsuzaki, H. Kishida, H. Okamoto, and Y. Tokura, Ultrafast Optical Switching to a Metallic State by Photoinduced Mott Transition in a Halogen-Bridged Nickel-Chain Compound, Phys. Rev. Lett. **91**, 057401 (2003).

[15] H. Okamoto, H. Matsuzaki, T. Wakabayashi, Y. Takahashi, and T. Hasegawa, Photoinduced Metallic State Mediated by Spin-Charge Separation in a One-Dimensional Organic Mott Insulator, Phys. Rev. Lett. **98**, 037401 (2007).

[16] V. R. Morrison, R. P. Chatelain, K. L. Tiwari, A. Hendaoui, A. Bruhács, M. Chaker, and B. J. Siwick, A photoinduced metal-like phase of monoclinic VO_2 revealed by ultrafast electron diffraction, Science **346**, 445 (2014).

[17] S. A. Dönges, O. Khatib, B. T. O'Callahan, J. M. Atkin, J. H. Park, D. Cobden, and M. B. Raschke, Ultrafast nanoimaging of the photoinduced phase transition dynamics in VO_2, Nano Lett. **16**, 3029 (2016).

[18] A. Takahashi, H. Itoh, and M. Aihara, Photoinduced insulator-metal transition in one-dimensional Mott insulators, Phys. Rev. B **77**, 205105 (2008).

[19] R. E. F. Silva, I. V. Blinov, A. N. Rubtsov, O. Smirnova, and M. Ivanov, High-harmonic spectroscopy of ultrafast many-body dynamics in strongly correlated systems, Nat. Photonics **12**, 266 (2018).

[20] T. Oka and H. Aoki, Photoinduced Tomonaga-Luttinger-like liquid in a Mott insulator, Phys. Rev. B **78**, 241104(R) (2008).

[21] T. Oka, Nonlinear doublon production in a Mott insulator: Landau-Dykhne method applied to an integrable model, Phys. Rev. B **86**, 075148 (2012).

[22] S. Ejima, F. Lange, and H. Fehske, Nonequilibrium dynamics in pumped Mott insulators, Phys. Rev. Res. **4**, L012012 (2022).

[23] Y. Murakami, S. Takayoshi, T. Kaneko, Z. Sun, D. Golež, A. J. Millis, and P. Werner, Exploring nonequilibrium phases of photo-doped Mott insulators with generalized Gibbs ensembles, Commun. Phys. **5**, 23 (2022).

[24] M. Eckstein, T. Oka, and P. Werner, Dielectric Breakdown of Mott Insulators in Dynamical Mean-Field Theory, Phys. Rev. Lett. **105**, 146404 (2010).

[25] M. Eckstein and P. Werner, Photoinduced States in a Mott Insulator, Phys. Rev. Lett. **110**, 126401 (2013).

[26] G. Mazza, A. Amaricci, M. Capone, and M. Fabrizio, Field-Driven Mott Gap Collapse and Resistive Switch in Correlated Insulators, Phys. Rev. Lett. **117**, 176401 (2016).

[27] D. Golež, M. Eckstein, and P. Werner, Dynamics of screening in photodoped Mott insulators, Phys. Rev. B **92**, 195123 (2015).

[28] J. Li and M. Eckstein, Nonequilibrium steady-state theory of photodoped Mott insulators, Phys. Rev. B **103**, 045133 (2021).

[29] B. Mayer, C. Schmidt, A. Grupp, J. Bühler, J. Oelmann, R. E. Marvel, R. F. Haglund, Jr., T. Oka, D. Brida, A. Leitenstorfer, and A. Pashkin, Tunneling breakdown of a strongly correlated insulating state in VO_2 induced by intense multiterahertz excitation, Phys. Rev. B **91**, 235113 (2015).

[30] H. Yamakawa, T. Miyamoto, T. Morimoto, T. Terashige, H. Yada, N. Kida, M. Suda, H. Yamamoto, R. Kato, K. Miyagawa *et al.*, Mott transition by an impulsive dielectric breakdown, Nat. Mater. **16**, 1100 (2017).

[31] L. Keldysh, Ionization in the field of a strong electromagnetic wave, Sov. Phys. JETP **20**, 1307 (1965).

[32] M. Y. Ivanov, M. Spanner, and O. Smirnova, Anatomy of strong field ionization, J. Mod. Opt. **52**, 165 (2005).

[33] C. Orthodoxou, A. Zaïr, and G. H. Booth, High harmonic generation in two-dimensional Mott insulators, npj Quantum Mater. **6**, 76 (2021).

[34] M. R. Bionta, E. Haddad, A. Leblanc, V. Gruson, P. Lassonde, H. Ibrahim, J. Chaillou, N. Émond, M. R. Otto, Á. Jiménez-Galán *et al.*, Tracking ultrafast solid-state dynamics using high harmonic spectroscopy, Phys. Rev. Res. **3**, 023250 (2021).

[35] F. H. L. Essler, H. Frahm, F. Göhmann, A. Klümper, and V. E. Korepin, *The One-Dimensional Hubbard Model* (Cambridge University Press, Cambridge, UK, 2005).

[36] C. A. Stafford and A. J. Millis, Scaling theory of the Mott-Hubbard metal-insulator transition in one dimension, Phys. Rev. B **48**, 1409 (1993).

[37] V. Gruson, L. Barreau, Á. Jiménez-Galan, F. Risoud, J. Caillat, A. Maquet, B. Carré, F. Lepetit, J.-F. Hergott, T. Ruchon *et al.*, Attosecond dynamics through a Fano resonance: Monitoring the birth of a photoelectron, Science **354**, 734 (2016).

[38] P. Rivière, R. Silva, and F. Martín, Pump-probe scheme to study the autoionization decay of optically-forbidden H_2 doubly excited states, J. Phys. Chem. A **116**, 11304 (2012).

[39] R. E. F. Silva, P. Rivière, and F. Martín, Autoionizing decay of H_2 doubly excited states by using xuv-pump–infrared-probe schemes with trains of attosecond pulses, Phys. Rev. A **85**, 063414 (2012).

[40] C. J. Joachain, N. J. Kylstra, and R. M. Potvliege, *Atoms in Intense Laser Fields* (Cambridge University Press, Cambridge, UK, 2009).

[41] M. P. M. Dean, Y. Cao, X. Liu, S. Wall, D. Zhu, R. Mankowsky, V. Thampy, X. M. Chen, J. G. Vale, D. Casa, J. Kim, A. H. Said, P. Juhas, R. Alonso-Mori, J. M. Glownia, A. Robert, J. Robinson, M. Sikorski, S. Song, M. Kozina *et al.*, Ultrafast energy- and momentum-resolved dynamics of magnetic correlations in the photo-doped Mott insulator Sr_2IrO_4, Nat. Mater. **15**, 601 (2016).

[42] G. Vampa, C. R. McDonald, G. Orlando, D. D. Klug, P. B. Corkum, and T. Brabec, Theoretical Analysis of High-Harmonic Generation in Solids, Phys. Rev. Lett. **113**, 073901 (2014).

[43] R. E. F. Silva, F. Martín, and M. Ivanov, High harmonic generation in crystals using maximally localized Wannier functions, Phys. Rev. B **100**, 195201 (2019).

[44] L. Yue and M. B. Gaarde, Introduction to theory of high-harmonic generation in solids: Tutorial, J. Opt. Soc. Am. B **39**, 535 (2022).

[45] T. Oka and H. Aoki, Ground-State Decay Rate for the Zener Breakdown in Band and Mott Insulators, Phys. Rev. Lett. **95**, 137601 (2005).

[46] Z. Lenarčič and P. Prelovšek, Ultrafast Charge Recombination in a Photoexcited Mott-Hubbard Insulator, Phys. Rev. Lett. **111**, 016401 (2013).

[47] U. D. Giovannini, S. A. Sato, H. Hübener, and A. Rubio, First-principles modelling for time-resolved ARPES under different pump–probe conditions, J. Electron Spectrosc. Relat. Phenom. **254**, 147152 (2022).